The Journal of Chemical Physics

RESEARCH ARTICLE | APRIL 07 2009

Electron scattering by trimethylene oxide, c-$(CH_2)_3O$, molecules

Czesław Szmytkowski; Alicja Domaracka; Paweł Możejko; Elżbieta Ptasińska-Denga

Check for updates

J. Chem. Phys. 130, 134316 (2009)
https://doi.org/10.1063/1.3108459

View Online
Export Citation
CrossMark

This article may be downloaded for personal use only. Any other use requires prior permission of the author and AIP Publishing. This article appeared in (citation of published article) and may be found at https://doi.org/10.1063/1.3108459

26 February 2024 10:59:09

AIP Publishing

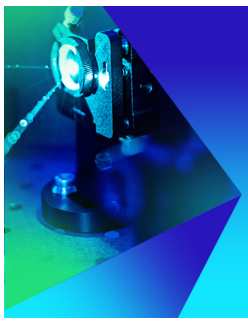

The Journal of Chemical Physics
Special Topic: Time-resolved Vibrational Spectroscopy
Submit Today
AIP Publishing

Electron scattering by trimethylene oxide, *c*-$(CH_2)_3O$, molecules

Czesław Szmytkowski,[a] Alicja Domaracka, Paweł Możejko, and Elżbieta Ptasińska-Denga
Atomic Physics Group, Faculty of Applied Physics and Mathematics, Gdańsk University of Technology, ul. G. Narutowicza 11/12, 80-233 Gdańsk, Poland

(Received 23 April 2008; accepted 8 March 2009; published online 7 April 2009)

Electron-scattering cross sections have been determined for trimethylene oxide, cyclic $(CH_2)_3O$ molecule, both experimentally and theoretically. The absolute total cross section (TCS) has been measured over energies from 1 to 400 eV using a linear electron-transmission method. The obtained TCS generally decreases with rising energy, except for the 3–10 eV range, where some resonantlike structures are discernible. Integral elastic cross section (ECS) and ionization cross section (ICS) have been also calculated up to 3 keV in the additivity rule approximation and the binary-encounter-Bethe approach, respectively. Their sum, ECS+ICS, is in a good agreement with the measured TCS. Comparison of the TCS energy dependence for trimethylene oxide with that for its isomeric open-chain counterpart—acetone, $(CH_3)_2CO$, has also been made. Moreover, examination of experimental TCSs for the cyclic $(CH_2)_nO$, $n=2-4$, ether series reveals that the intermediate-energy molecular TCSs for members of that family can be nicely represented as a sum of the effective TCSs for particular constituents of the molecule, i.e., methylene groups and oxygen atom. Finally, based on these partial TCSs, the TCS for the *c*-$(CH_2)_5O$—the next member of the series—has been determined and compared with the respective ECS+ICS values computed here for this compound. © *2009 American Institute of Physics*. [DOI: 10.1063/1.3108459]

I. INTRODUCTION

Comprehensive sets of measurables concerning elementary electron-assisted phenomena for a wide variety of compounds[1] are indispensable in many areas of science and nowadays technology.[2,3] Despite a long tradition and great experimental and theoretical efforts, the status of available electron-molecule scattering cross sections, electron transport, and rate coefficients is still not satisfactory. Deficiency of data describing the scattering processes is partly due to experimental difficulties with more complex and/or unstable compounds. On the other hand, the multicenter nature of the electron-molecule scattering makes the solution of the full scattering problem very demanding. Therefore, it seems valuable to search for correlations of scattering quantities with constitutive target parameters. When found, such correlations provide some stimulatory insight into the role of target properties in the scattering process, while the semiempirical formula describing these correlations would allow to estimate cross sections lacking in experimental data or calculations. The search of trends in cross sections requires, however, reliable experimental results for properly chosen series of targets—if possible, the data should be taken with the same experimental setup.

The present work is one in an extended series of our systematical studies focused on determining the total electron-scattering absolute cross sections (TCSs) for polyatomic compounds over a wide energy range. The main objective of this work is to provide accurate absolute TCS for the electron scattering from trimethylene oxide, *c*-$(CH_2)_3O$, molecule—a member of cyclic ethers family *c*-$(CH_2)_nO$. From 1 to 400 eV absolute TCS values are obtained in the electron-transmission experiment. To extend the data beyond the experimental range, up to 3 keV, approximate calculations are employed. The present TCS data for *c*-$(CH_2)_3O$ along with our recent results for *c*-$(CH_2)_2O$ and *c*-$(CH_2)_4O$ enable us to search how the cross section changes across this heterocyclic series. Neither experimental nor theoretical results concerning the electron-induced processes in trimethylene oxide have been reported in the literature as yet.

II. EXPERIMENT

To measure the absolute TCS, we have employed the electron-transmission method in a linear configuration. The electron spectrometer setup and procedures used in this work are essentially similar to those exploited in our recent TCS experiments,[4] therefore we present here a brief outline only. An electron beam of required energy E ($\Delta E \leq 0.1$ eV, full width at half maximum) was prepared by the electron optics system equipped with an electron gun, a cylindrical 127° electrostatic monochromator, and set of electron lenses. The collimated beam of electrons was then directed into a reaction chamber filled with a sample vapor. The projectiles which passed the exit chamber slit were energetically discriminated with the retarding field lens system, and eventually collected by a Faraday cup.

The method relates the transmission of the target for a beam of electrons to the total electron-scattering cross section, $Q(E)$, by the Bouguer–de Beer–Lambert (BBL) attenuation formula,

[a]Electronic mail: czsz@mif.pg.gda.pl.

 © 2009 American Institute of Physics

MOST WIEDZY Downloaded from mostwiedzy.pl
26 February 2024 10:59:09

$$I(E,p) = I(E,0)\exp\left[-\frac{pl}{k\sqrt{T_t T_m}}Q(E)\right],$$

where $I(E,p)$ and $I(E,0)$ are the transmitted electron intensities measured in the presence and absence of the target molecules in the scattering cell; l refers to the effective path length of electrons through the target—here assumed equal to a linear distance (=30.5 mm) between entrance and exit slits of the collision cell; k is the Boltzmann constant. The target pressure p was measured with the Baratron capacitance manometer head stabilized at 322 K ($=T_m$). As the temperature of the target T_t (in fact, of the scattering chamber) is usually lower than T_m by 5–10 K and varies slowly in course of the experiment, the pressure readings are corrected for the thermal transpiration effect.[5] The background pressure in the electron optics volume was kept constant, at the level of about three orders lower than the target pressure in the scattering cell. The electron energy scale was calibrated by reference to the oscillatory structure observed around 2.3 eV in the transmitted current after the admixture of N_2.

The resulting absolute TCS value at each impact energy was determined as weighted mean of results from several series performed at slightly different electron optics settings and for target pressures ranging from about 25 to 150 mPa; the pressures applied ensure the single-collision conditions in the scattering volume. The TCS uncertainty of a random nature (one standard deviation of the weighted mean TCS value) does not exceed 1% over the whole energy range investigated. The overall TCS uncertainty is, however, dominated by possible systematic uncertainties which may appear while taking the individual quantities necessary for the TCS determination from the BBL formula.[6,7] Main contributions to the systematic TCS error come from (i) the inability to discriminate against electrons which are scattered elastically through small angles ($<2°$) in the forward direction—this effect may systematically lower the measured TCS by 4% near 1 eV; (ii) the effusion of the target molecules through orifices of the scattering cell that leads to inhomogeneity of target density in the reaction volume and to elongation of the effective path over which the scattering events take place;[8] (iii) the shift in the energy scale observed during the experiment, by nearly 0.1 eV—especially troublesome below 2 eV where the TCS raises steeply. These errors can be estimated roughly only and the final TCS results are not corrected for above-mentioned effects. The overall systematic uncertainty in our measured absolute TCS amounts up to 8%–10% below 2 eV, 4%–6% within 4–100 eV, and 6%–8% at higher energies applied. The sample of trimethylene oxide (99.5 +%), commercially supplied by Aldrich, was used after vacuum distillation.

III. COMPUTATIONAL DETAILS

The main goal of the present computations is to obtain reasonable estimates of TCS, as sum of elastic cross sections (ECSs) and ionization cross sections (ICSs), for two cyclic ethers: c-$(CH_2)_3O$ and c-$(CH_2)_5O$, for energies at which experiments have not been performed.

Elastic cross sections (ECSs) for electron collisions with molecules studied, c-$(CH_2)_3O$ and c-$(CH_2)_5O$, have been calculated with the independent atom method[9] (IAM) while electron-impact ICSs have been obtained within the binary-encounter-Bethe[10] (BEB) formalism.

In the IAM approximation the integral ECS for electron scattering from a molecule is given by

$$\sigma^{\mathrm{el}}(E) = \frac{4\pi}{k}\sum_{i=1}^{N} \mathrm{Im}\, f_i(\theta=0,k) = \sum_{i=1}^{N}\sigma_i^A(E),$$

where $f_i(\theta,k)$ is the scattering amplitude due to the ith atom of the target molecule, θ is the scattering angle, while E and $k=\sqrt{2E}$ stand for energy and the wave number of the incident electron, respectively. The ECS for the ith atomic constituent of the molecule, $\sigma_i^A(E)$, has been derived according to

$$\sigma^A = \frac{4\pi}{k^2}\left(\sum_{l=0}^{l_{\max}}(2l+1)\sin^2\delta_l + \sum_{l=l_{\max}}^{\infty}(2l+1)\sin^2\delta_l^{(B)}\right).$$

To obtain phase shifts δ_l, partial wave analysis has been employed and the radial Schrödinger equation,

$$\left[\frac{d^2}{dr^2} - \frac{l(l+1)}{r^2} - 2(V_{\mathrm{stat}}(r) + V_{\mathrm{polar}}(r)) + k^2\right]u_l(r) = 0,$$

has been solved numerically under the boundary conditions

$$u_l(0) = 0, \quad u_l(r) \overset{r\to\infty}{\to} A_l\hat{j}_l(kr) - B_l\hat{n}_l(kr),$$

where $\hat{j}_l(kr)$ and $\hat{n}_l(kr)$ are the Riccati–Bessel and Riccati–Neumann functions, respectively. Our previous intermediate-energy studies (e.g., Ref. 11) have shown that the IAM method, with only the static and polarization parts of the electron-target interaction, reproduces experimental elastic integral cross sections satisfactorily. Therefore, in the present calculations the electron-atom interaction has been represented just by sum of the static, $V_{\mathrm{stat}}(r)$,[12] and polarization, $V_{\mathrm{polar}}(r)$,[13] potentials, which are given by following expressions:

$$V_{\mathrm{stat}}(r) = -\frac{Z}{r}\sum_{m=1}^{3}\gamma_m\exp(-\beta_m r),$$

where Z is the nuclear charge of the atom and γ_m and β_m are parameters obtained by fitting to the numerical Dirac–Hartree–Fock–Slater screening function,[12]

$$V_{\mathrm{polar}}(r) = \begin{cases} \nu(r), & r \le r_c \\ -\alpha/2r^4, & r > r_c, \end{cases}$$

where $\nu(r)$ is the free-electron-gas correlation energy,[14] α is the static electric dipole polarizability of atom, and r_c is the first crossing point of the $\nu(r)$ and $-\alpha/2r^4$ curves.[15]

The phase shifts δ_l are connected with asymptotic form of the wave function $u_l(r)$ by

$$\tan\delta_l = \frac{B_l}{A_l}.$$

In the present calculations the exact phase shifts have been calculated for l up to $l_{\max}=50$ while those remaining, $\delta_l^{(B)}$, have been included through the Born approximation.

MOST WIEDZY Downloaded from mostwiedzy.pl

26 February 2024 10:59:09

Within the BEB model the electron-impact ICS for given molecular orbital is expressed by formula[10]

$$\sigma^{\mathrm{BEB}} = \frac{S}{\epsilon + u + 1}\left[\frac{\ln \epsilon}{2}\left(1 - \frac{1}{\epsilon^2}\right) + 1 - \frac{1}{\epsilon} - \frac{\ln \epsilon}{\epsilon + 1}\right],$$

where $S = 4\pi a_0^2 N R^2 / B^2$ ($a_0 = 0.5292$ Å, $R = 13.61$ eV), $u = U/B$, $\epsilon = E/B$, and E is the energy of impinging electrons. The total cross section σ^{ion} for electron-impact ionization of molecule can be obtained as the sum of ICSs for all molecular orbitals, i.e.,

$$\sigma^{\mathrm{ion}} = \sum_{j=1}^{n_{\mathrm{MO}}} \sigma_j^{\mathrm{BEB}},$$

where n_{MO} is the number of molecular orbitals.

The advantage of the BEB model is that all quantities necessary to calculate ICS have the exact physical meaning and can be evaluated with standard quantum chemistry methods. In the present work the electron binding energy B, kinetic energy of the orbital, U, and the orbital occupation number N, have been calculated for the geometrically optimized c-$(CH_2)_3O$ and c-$(CH_2)_5O$ molecules with the Hartree–Fock method using the GAUSSIAN code[16] and the Gaussian 6–311G basis set. Energies of the highest occupied molecular orbitals obtained this way differ usually from the experimental values, therefore we also performed outer valence Green function calculations of correlated electron affinities and ionization potentials[17–20] using the same GAUSSIAN code.

The sum of the ECS and ICS calculated for examined targets makes it possible to estimate the theoretical total cross sections for electron scattering by c-$(CH_2)_3O$ and c-$(CH_2)_5O$ molecules—the quantities used for further comparisons.

IV. RESULTS AND DISCUSSION

In this section we report on the absolute TCS measured for trimethylene oxide, c-$(CH_2)_3O$, molecule. The measurements have been carried out in the linear transmission experiment over energy range from 1 to 400 eV. We present also our electron-impact integral ECS and ICS computed, both up to 3 keV, in the additivity rule approximation and the BEB approach, respectively. The sum of ECS and ICS calculated at intermediate energies is then compared with the measured TCS. We compare also TCSs for cyclic trimethylene oxide and for its isomeric open-chain counterpart—acetone—to search how the arrangement of atoms in c-$(CH_2)_3O$ and $(CH_3)_2CO$ reflects in cross section for electron scattering. Furthermore, we confront our experimental TCSs for three heterocyclic $(CH_2)_nO$, $n=2-4$, homologies. Similarities and differences of TCS energy functions are pointed out and discussed. We have found, based on these observations, that the intermediate-energy TCS for members of this heterocyclic series can be thought of as a sum of corresponding submolecular TCS terms. Partitioning of TCS for c-$(CH_2)_nO$, $n=2-4$, molecules has been carried out to find effective TCS contributions from the methylene group and oxygen atom. Finally, the electron-scattering TCS for the c-$(CH_2)_5O$ is estimated and compared with our cross section (elastic+ionization) computations.

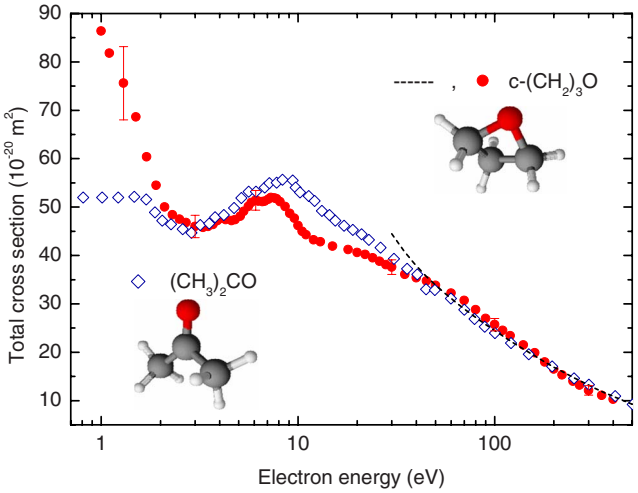

FIG. 1. (Color online) Cross sections for electron scattering from C_3H_6O molecules. The present results for the ring isomer, c-$(CH_2)_3O$: Experimental (full circles) absolute TCSs, error bars denote overall (systematic +statistical) uncertainties; sum (dashed line) of computed integral ECS, and ICS. To show the isomer effect, the experimental results (open diamonds) for the open-chain isomer, $(CH_3)_2CO$, from Ref. 24 are also presented. Molecule pictographs are included.

A. Trimethylene oxide, c-$(CH_2)_3O$

Figure 1 shows the experimental TCS for electron scattering by C_3H_6O molecules as a function of impact energy, in the range from 1 to 400 eV. The absolute TCS values for a ring $(CH_2)_3O$ molecule versus energy are listed in Table I. The general observation is that the magnitude of the TCS for c-$(CH_2)_3O$ is relatively high over the whole energy range investigated that, except the lowest energies, reflects the rather large geometrical size of the molecule.

According to the appearance of the measured e^--$(CH_2)_3O$ TCS energy dependence, presented in Fig. 1, several interesting features are worth noting. Starting from 1 eV the TCS energy function rapidly decreases from nearly 86×10^{-20} m^2 to its local minimum of about 46×10^{-20} m^2 near 3.3 eV and, respecting this trend, closely resembles a general low-energy TCS behavior observed for other polar targets. As the c-$(CH_2)_3O$ molecule has relatively high electric dipole moment ($\mu = 1.94$ D, cf. Table II), such TCS low-energy appearance may be explained in terms of direct scattering of the point charge on the long-range dipole potential,[21] although, a contribution from the induced polarization effects ($\alpha \sim 6 \times 10^{-30}$ m^3, Table II) should also be considered. Behind the minimum, the TCS shows a distinct broad enhancement spanned between 5 and 12 eV. It is composed of two overlapping structures, peaking near 6 and 7.5 eV with the value of about 52×10^{-20} m^2, as indicated in Fig. 1. However, at the left-hand foot of the enhancement, near 4.1 eV, another weak maximum of about 48×10^{-20} m^2 appears. We suggest the resonant origin of these three structures, although, we do not have direct evidence for such statement; the ground is based only on the observations

MOST WIEDZY Downloaded from mostwiedzy.pl
26 February 2024 10:59:09

TABLE I. Absolute TCSs measured for electron impact on trimethylene oxide molecules, c-$(CH_2)_3O$, in units of 10^{-20} m^2.

Energy (eV)	TCS	Energy (eV)	TCS	Energy (eV)	TCS	Energy (eV)	TCS
1.0	86.4	4.8	47.4	10.5	45.0	80	28.8
1.1	81.8	5.1	48.1	11	44.3	90	27.5
1.3	75.6	5.3	49.1	12	43.2	100	25.7
1.5	68.6	5.6	50.1	13	42.8	110	24.5
1.7	60.4	5.8	50.9	15	41.9	120	23.4
1.9	54.5	6.1	51.4	18	41.2	140	21.5
2.1	50.0	6.3	51.2	20	40.6	160	19.9
2.3	48.4	6.6	51.1	22	40.2	180	18.0
2.5	47.5	6.8	51.2	24	39.5	200	16.5
2.7	46.8	7.1	51.6	26	38.8	220	15.3
3.0	46.0	7.3	52.0	28	38.1	250	14.0
3.3	45.8	7.6	51.9	30	37.6	270	13.2
3.5	46.0	7.8	51.7	35	36.1	300	12.1
3.7	46.4	8.1	51.1	40	35.4	350	11.1
3.9	47.2	8.6	50.1	45	34.7	400	10.3
4.1	47.7	9.1	48.7	50	33.8		
4.3	47.4	9.6	47.7	60	32.2		
4.6	47.2	10	46.2	70	30.7		

for other hydrocarbons in this energy regime (e.g., Ref. 22). A resonance may arise when the approaching electron of appropriate energy attaches to the target molecule creating a molecular negative-ion state for a time interval long compared to the electron passage time. Subsequently, the resulting transient anion can decompose via autodetachment of the extra electron or through decay into negative stable fragment and neutrals. Above approximately 10 eV the TCS energy function decreases with the energy increase, but between 15 and 25 eV some change in the slope is discernible. This broad feature may be also attributed to numerous weak resonant structures which overlap in this energy range, but it may arise as well due to nonresonant inelastic processes, mainly ionization. Beyond 30 eV the experimental TCS monotonically decreases down to about 10×10^{-20} m^2 near 400 eV. Present computations show (cf. Table III) that while around 400 eV the elastic and ionization contributions to the TCS are nearly equal, in the vicinity of the ICS maximum (70–100 eV) the ECS exceeds the ionization one by a factor of 1.5.

TABLE II. Summary of molecular electric dipole moments μ, electric dipole polarizabilities α, and the gas-kinetic cross sections σ_{gk} for cyclic $(CH_2)_nO$ series, $n=2-5$.

Molecule	μ (D)[a]	α (10^{-30} m^3)	σ_{gk} (10^{-20} m^2) [b]
c-$(CH_2)_2O$	1.89	4.43[a]	11.2
c-$(CH_2)_3O$	1.94	6.1[c]	13–14[d]
c-$(CH_2)_4O$	1.63[e], 1.75	8.0[c]	15.3
c-$(CH_2)_5O$	1.58	9.8[c]	16.8

[a]Reference 31.
[b]Estimated from van der Waals constant b (Ref. 31).
[c]Estimation based on the additivity formula from Ref. 44.
[d]This work.
[e]Reference 43.

Figure 1 also compares our TCS measurements with the sum of calculated ECS and ICS for trimethylene oxide (see Table III), which stands for the theoretical TCS estimation. Above 45 eV the agreement between the experiment and calculations is good, both with respect to the shape and magnitude. The differences do not exceed 3%–7%, falling within typical experimental uncertainty limits. Such an agreement entitles us to believe that our high-energy ECS+ICS values, calculated at energies beyond the experimental regime, represent the TCS equally well as these at intermediate energies.

Finally, proximity of intermediate-energy TCSs and respective gas-kinetic cross sections, noticed earlier (see Ref. 23, and references therein), allowed us to estimate the σ_{gk} value for trimethylene oxide molecule (Table II).

B. Comparison between c-$(CH_2)_3O$ and $(CH_3)_2CO$: The isomer effect

Figure 1 compares also the current TCS results for trimethylene oxide, a ring molecule, with the data (from Ref. 24) for its isomeric open-chain counterpart—acetone, which is composed of two methyl groups, CH_3, and one carbonyl group, C=O.

It is clearly seen from Fig. 1 that the change in the arrangement of atoms in target molecule (*isomer effect*) manifests mainly in the magnitude of TCS at energies below 40 eV. Within 4–40 eV the TCS for the cyclic C_3H_6O isomer is noticeably lower than the TCS for its open-chain analog. The same behavior has been already observed for the pair of C_3H_6 isomers, cyclopropane, and propene.[25–28] It is interesting that the shape of TCSs for c-$(CH_2)_3O$ and for $(CH_3)_2CO$ is basically similar, except for the energy range below 1.4 eV. Both TCS curves have a minimum near 3 eV, three weak narrow features located close to 4, 6, and 8–9 eV, and a broad enhancement spanned between 5 and 15 eV. Above 10 eV the examined TCS functions decrease rather monotoni-

26 February 2024 10:59:09

MOST WIEDZY Downloaded from mostwiedzy.pl

TABLE III. ICS and integral ECS calculated for electron impact on c-$(CH_2)_3O$ and c-$(CH_2)_5O$ molecules, in 10^{-20} m^2.

E	ICS		E	ICS		ECS	
(eV)	$(CH_2)_3O$	$(CH_2)_5O$	(eV)	$(CH_2)_3O$	$(CH_2)_5O$	$(CH_2)_3O$	$(CH_2)_5O$
9.342		0	30	6.41	10.2	38.0	59.0
9.659	0		35	7.44	11.8	33.2	51.6
10	0.033	0.071	40	8.19	13.0	29.6	46.1
11	0.141	0.214	45	8.75	13.8	26.9	41.8
12	0.326	0.478	50	9.16	14.4	24.7	38.5
13	0.586	0.885	60	9.64	15.1	21.4	33.4
14	0.879	1.42	70	9.85	15.4	19.1	29.7
15	1.23	2.01	80	9.89	15.4	17.3	27.0
16	1.63	2.65	90	9.84	15.3	15.9	24.8
17	2.03	3.36	100	9.72	15.1	14.8	23.0
18	2.46	4.06	110	9.56	14.8	13.8	21.5
19	2.89	4.74	120	9.38	14.5	13.0	20.2
20	3.29	5.37	140	8.99	13.9	11.7	18.1
22.5	4.22	6.83	160	8.60	13.3	10.6	16.5
25	5.04	8.12	180	8.21	12.7	9.78	15.2
27.5	5.77	9.25	200	7.85	12.1	9.08	14.1
			300	6.40	9.80	6.79	10.5
			400	5.40	8.24	5.48	8.44
			500	4.67	7.13	4.62	7.09
			600	4.13	6.29	4.00	6.13
			700	3.70	5.64	3.53	5.41
			800	3.36	5.11	3.17	4.84
			900	3.08	4.69	2.87	4.39
			1000	2.85	4.33	2.63	4.02
			2000	1.65	2.50	1.51	2.30
			3000	1.18	1.79	1.24	1.91

cally with rising energy, and beyond 40 eV they merge, confirming earlier findings that above 40–50 eV the isomers are not distinguishable with respect to the TCSs.[27,29] Such behavior of TCS for isomers means that the energy of 40–50 eV stands for the lower limit above which TCS becomes insensitive to geometrical rearrangement of atoms in the target molecule, and the IAM becomes applicable. That conclusion is also confirmed by our earlier IAM calculations.[23,30]

Considering again the low impact energies, it is somewhat surprising that below 2 eV, the TCS for acetone,[24] a molecule with a substantially higher dipole moment ($\mu_{(CH_3)_2CO}$=2.9 D; $\mu_{(CH_2)_3O}$=1.9 D),[31] is distinctly lower (cf. Fig. 1) than that for trimethylene oxide. Moreover, the mean scattering cross section for acetone is about 3×10^{-17} m^2 at thermal energies,[32] therefore one would expect a steep increase in TCS, at least below 1 eV. To elucidate the low-energy cross section behavior for $(CH_3)_2CO$, further experiments are necessary around 1 eV.

C. Comparison of electron-scattering TCSs for cyclic-$(CH_2)_nO$, n=2–5, homologies: Group additivity rule

So far, we have been interested in how the TCS for the c-$(CH_2)_3O$ molecule varies with the energy of the impinging electron. In this subsection we are concerned with the variation of the TCS from target to target going across the family of cyclic ethers $(CH_2)_nO$ (n=2–4) in order to find how the change in the number of CH_2 groups in the molecule is reflected in its TCS curve.

The considered molecules are heterocyclic organic compounds composed of n methylene groups with one oxygen atom embedded in the C–C ring (see Fig. 2). The presence of the oxygen atom results in a considerable asymmetry of the electric charge distribution and, in consequence, leads to a distinct electric dipole moment of the molecule (Table II).

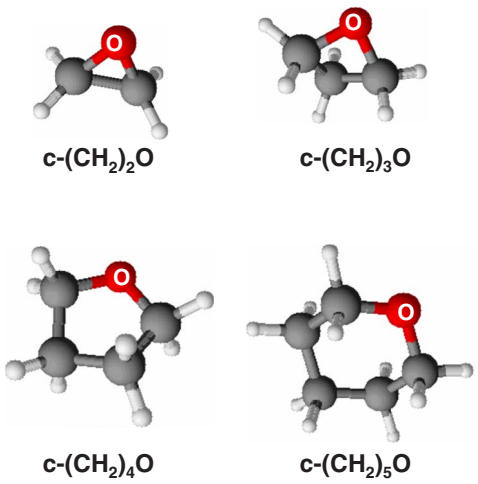

FIG. 2. (Color online) Schematic geometry of the heterocyclic $(CH_2)_nO$ molecules, n=2–5.

MOST WIEDZY Downloaded from mostwiedzy.pl

26 February 2024 10:59:09

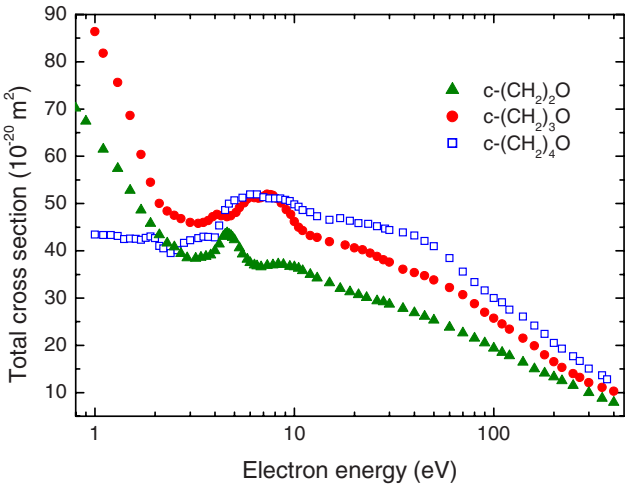

FIG. 3. (Color online) Comparison of experimental TCSs for electron scattering on c-$(CH_2)_2O$ (full triangles), from Ref. 33; c-$(CH_2)_3O$ (full circles), present; c-$(CH_2)_4O$ (open squares), from Ref. 30.

In Fig. 3, the experimental TCSs for electron impact on three members of the c-$(CH_2)_nO$, $n=2-4$, molecular family are compared at energies from about 1 to 400 eV. The comparison is made based on the TCSs measured in our laboratory: c-$(CH_2)_2O$ (Ref. 33), c-$(CH_2)_3O$ present, and c-$(CH_2)_4O$ (Ref. 30). Considering the shape of TCS curves and the relation of the TCS magnitudes, the examined energy range can be divided into three regions: Below 2.5 eV, between 2.5 and 9 eV, and beyond 9 eV.

An inspection of the low-energy experimental TCSs for considered $(CH_2)_nO$ molecules (Fig. 4) reveals some noteworthy features: (i) Below 2.5 eV the magnitude of the measured TCSs cannot be correlated with the molecular size of the respective target (cf. Ref. 31); (ii) in this energy range the TCS magnitudes change rather in order of the electric dipole moment of molecules (see Table II)—the higher is the molecular dipole moment, the higher is the low-energy TCS of the molecule; (iii) the experimental low-energy TCS appears to be more steeply decreasing function for the target with higher dipole moment. Within 1–2.5 eV the TCS for c-$(CH_2)_3O$ ($\mu=1.94$ D) decreases almost twofold with the energy increase, for c-$(CH_2)_2O$ ($\mu=1.89$ D) by a factor of 1.5, while for c-$(CH_2)_4O$ ($\mu=1.7$ D) the measured TCS decreases only by a few percent. Figure 4 confronts also the behavior of our experimental low-energy TCSs for electron scattering on the cyclic $(CH_2)_nO$, $n=2-4$, molecules with the theoretical predictions based on the point-dipole Born angle-differential cross section formula developed by Altshuler.[34] To mimic our transmission experiment, in which the electrons scattered elastically at small angles into the forward direction are not distinguishable from those not scattered, the Born angular distributions (from Ref. 34) are integrated over the angles $2° \leq \theta \leq 180°$, out of the forward direction acceptance angle of the electron detector (see Sec. II). The resulting Born integral cross sections (BCSs) rise toward low electron-impact energies like E^{-1} and change with the electric dipole moment μ of molecule, as μ^2. Figure 4 clearly shows that with respect to the slope of the low-energy cross section curve, there is a discrepancy between

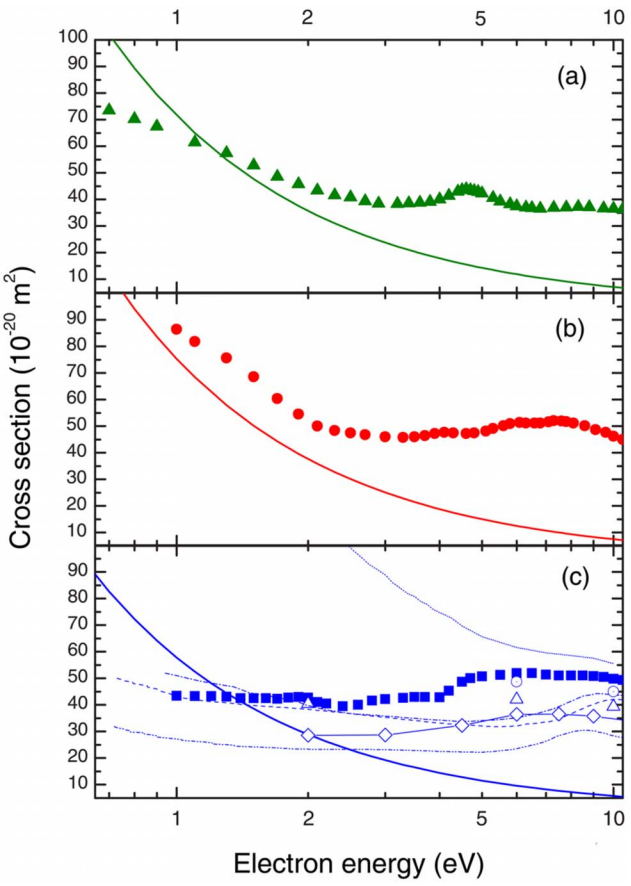

FIG. 4. (Color online) Cross sections for low-energy electron scattering from the cyclic $(CH_2)_nO$, $n=2-4$, molecules. (a) c-$(CH_2)_2O$: (full triangles), TCS experimental from Ref. 33; (solid line), calculated integral BCS, see the text, present. (b) c-$(CH_2)_3O$: (full circles), TCS experimental, present; (solid line), calculated BCS, present. (c) c-$(CH_2)_4O$. Experimental: (full squares), TCS from Ref. 30; (open diamonds), TCS from Ref. 35, line through experimental points is added to guide the eye; (open circles), total (elastic+vibrational) from Ref. 36; (open triangles), elastic from Ref. 36; Theoretical: (dot line), elastic plus electronically inelastic (using the R-matrix method, with Born correction) from Ref. 39; (dot-dash line), elastic (using the R-matrix method) from Ref. 40; (dot-dot-dash line), momentum transfer cross section (using the complex Kohn variational method) from Ref. 37; (dash line), elastic (using the Schwinger multichannel method, without explicit correction for the point-dipole interaction) from Ref. 38; (solid line), BCS, present.

the Born predictions and the experimental TCSs. Quite unexpectedly, the discrepancy increases as the electric dipole moment of examined molecule decreases. While the variation in the TCS at low energies for c-$(CH_2)_3O$ [see Fig. 4(b)] is generally consistent with the respective BCS, for c-$(CH_2)_2O$ the slope of the TCS curve is evidently less steep than the BCS [Fig. 4(a)], and the behavior of the experimental TCS for c-$(CH_2)_4O$ molecule does not follow the Born predictions at all [cf. Fig. 4(c)]. The origin of this effect is unclear because the lowering of the measured TCS—due to incomplete discrimination of forwardly scattered electrons—should rather decrease with the decrease in the target dipole moment. Looking for any arguments, we inspected other known low-energy experimental and theoretical data, also included in Fig. 4(c). The shape of the low-energy TCS curve[30] for the c-$(CH_2)_4O$ appeared to be rather similar to earlier TCS measurements of Zecca *et al.*[35] and to integral

26 February 2024 10:59:09

MOST WIEDZY Downloaded from mostwiedzy.pl

elastic data cross sections taken recently by Allan[36] (note an excellent agreement in the magnitude of the TCS from Ref. 30 with the elastic+inelastic data of Allan); it does not differ much from that in the momentum transfer and elastic integral cross sections calculated by Trevisan *et al.*[37] and by Winstead and McKoy,[38] respectively. On the other hand, the recent *R*-matrix calculations of Bouchiha *et al.*[39] and of Tonzani and Greene[40] clearly show more steep rise of the cross section curve below 2.5 eV. Considering the above, we can speculate that the electron-scattering cross section for tetrahydrofuran increases toward thermal energies, as it would for polar target, but the increase is less steep than the Born cross section and it becomes more distinct only below 1 eV. Nevertheless, further studies of the low-energy TCS behavior for the cyclic ethers are desired.

More difficult to grasp are regularities in TCSs behavior within 3–12 eV, where TCS varies irregularly and rather unforeseeable with electron energy. In this energy range subtle resonant effects become to play a significant role and more detailed properties of the target are exposed. However, some common features can be observed in Figs. 3 and 4, and they are pointed out below.

(i) Between 3 and 5 eV the TCS for all considered molecules exhibits a more or less distinct maximum located around 4.6 eV for c-$(CH_2)_2O$, 4.2 eV for c-$(CH_2)_3O$, and 3.6 eV for c-$(CH_2)_4O$. The maximum becomes noticeably weaker and it shifts to lower energies with increasing size of the molecular ring. In the case of c-$(CH_2)_2O$, the 4.6 eV TCS maximum[33] was related to resonant structure observed earlier in the vibrational spectra[22] and associated with the electron-impact excitation of the C–C ring stretch mode. The decreasing intensity of the maximum across the c-$(CH_2)_nO$ family may suggest that the resonant excitation of C–C stretching within 3 and 5 eV becomes less effective with the increase in the ring, as it becomes less rigid. Indeed, recent vibrational spectra for gas-phase c-$(CH_2)_4O$ do not reveal an excitation of the C–C mode below 4 eV; instead, near 2.6 eV a weak feature coupled to excitation of the CH_2 scissoring vibration was observed and associated with the formation of a shape resonance.[36] On the other hand, the excitation of the C–C stretching vibrational mode around 3.5 eV has been noticed in condensed c-$(CH_2)_4O$.[41]

(ii) Another structure, common for the compared TCSs, is the broad enhancement located between 7 and 16, 5 and 14, and 4 and 15 eV, for molecules with two, three, and four methylene groups, respectively. In the range of the TCS enhancement the resonant excitation of the methylene group was observed for c-$(CH_2)_2O$ and c-$(CH_2)_4O$ molecules.[22,36,42] The distinct increase in the enhancement magnitude with the increase in the number of the CH_2 groups can be, therefore, explained in terms of the resonant excitation of vibrational modes of molecules in this energy range. One can also notice that the outset of this enhancement shifts to lower energies with increasing number of CH_2 groups in the considered molecule, and the extra structures on its edge become more visible. Regarding general appearance, behind 6–7 eV the TCS for the heterocyclic molecules essentially resembles the TCSs for respective carbon-cyclic targets—in this energy range the TCS practically does not alter if one CH_2 group is replaced with an oxygen atom (e.g., Ref. 33).

Above 9 eV the TCS energy curves for c-$(CH_2)_nO$, $n=2-4$, molecules behave similarly to each other—they monotonically decrease when energy increases, with some shoulder apparent within 20–40 eV; this structure becomes more noticeable when the number of CH_2 groups in molecule increases. It is also evident that the target of the larger molecular size has distinctly higher TCS. For electron-impact energies between 80 and 400 eV, the energy dependence of our TCSs measured for c-$(CH_2)_nO$, $n=2-4$, molecules can be reasonably described with the easy-to-apply function $\sim E^{-a}$, where $a \simeq 0.6$. The same function reproduces, to a good approximation, our calculated total (elastic+ionization) cross sections. In the high-energy limit, the total cross section for the electron scattering can be expressed with a combined Born–Bethe (BB) formula,

$$\sigma_{(\mathrm{el+inel})}^{\mathrm{BB}} = A_1 \frac{R}{E} + A_2 \left(\frac{R}{E}\right)^2 + B \frac{R}{E} \ln\left(C \frac{E}{R}\right) + \cdots,$$

where E is the incident energy; $R=13.61$ eV; A, B, and C are constants related to the target properties.[45] Recent investigations[46] for molecules show, however, that the BB approximation agrees well with the experimental TCS values only far beyond 4–5 keV. The difference between measurements and the BB theory may partly result from experimental problems related to an insufficient discrimination against the electrons scattered into the forward direction and against the main inelastic channels (see Sec. II). The appropriate corrections of TCS values lower, but do not eliminate, the discrepancies; in the vicinity of 2 keV the experimental points lie about 25% below the BB theory predictions, and this difference substantially increases toward low-intermediate energies. Therefore, to fit the intermediate-energy TCSs for series of molecules, some semiempirical formulas have been proposed, usually containing the E^{-a} factor, with $a=0.5-1.0$.[25,26,46–49]

A closer inspection of the electron-scattering data for c-$(CH_2)_nO$ series reveals that above 20 eV the TCS for c-$(CH_2)_3O$ is in excellent agreement with the arithmetic mean of TCSs for two nearest homologies, c-$(CH_2)_2O$ and c-$(CH_2)_4O$ (see Fig. 5). It means that the TCS at intermediate energies increases in direct proportion to the number of CH_2 groups in the molecule. That implies that at higher energies the TCS for complex molecule may be estimated with a reasonable accuracy using the TCSs of its submolecular components and/or from the TCSs for simpler compounds (*group additivity rule*). This observation corresponds with earlier findings,[23,27,50] that for energies above 30–40 eV, where resonant effects become weak and can be neglected, the kind of target components and their count are more important in the

MOST WIEDZY Downloaded from mostwiedzy.pl

26 February 2024 10:59:09

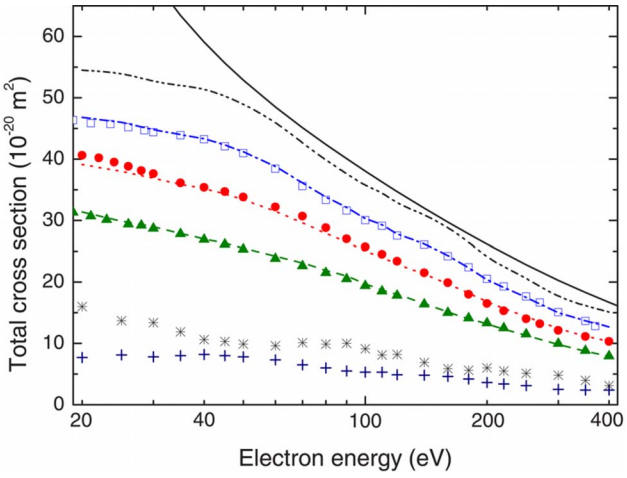

FIG. 5. (Color online) Comparison of the experimental and/or calculated TCSs with these estimated from the partitioning scheme (see text, Sec. IV C) for the electron scattering from cyclic $(CH_2)_nO$ (n=2–5) molecules. Experimental: c-$(CH_2)_2O$ (full triangles), from Ref. 33; c-$(CH_2)_3O$ (full circles), present; c-$(CH_2)_4O$ (open squares), from Ref. 30. Estimated, present: Oxygen atom (asterisks); CH_2 (crosses); c-$(CH_2)_2O$ (dash line); c-$(CH_2)_3O$ (dot line); c-$(CH_2)_4O$ (dot-dash line); c-$(CH_2)_5O$ (dot-dot-dash line). Calculated: Sum of ECSs and ICSs, $(CH_2)_5O$ (solid line), present.

electron-molecule scattering than the arrangement of the components in the molecule.

Based on the experimental TCS data for the c-$(CH_2)_nO$ (n=2–4) series one can estimate the effective TCS associated with the CH_2 group and oxygen atom in these molecules. Figure 5 shows the energy dependence of the effective TCS derived for these constituents. Note that within 20–100 eV, where some data are available, the evaluated contribution of oxygen atom to the molecular TCS for c-$(CH_2)_nO$ compounds is almost 1.5 times of the TCS for electron scattering from free oxygen atom,[51] while that estimated for CH_2 group is at 30 eV by the same factor lower than that calculated for free methylene radical.[10,52] Having in hand effective partial TCS values, one can attempt to estimate the intermediate-energy TCS dependence for tetrahydropyran, the next member (n=5) of the cyclic $(CH_2)_nO$ family. Figure 5 presents also the TCS estimated in this way for the c-$(CH_2)_5O$ molecule and compares it with our computations based on the ECS and ICS calculations. Above 40 eV the calculated total cross section (ECS+ICS) is consistently higher by 3%–11% than the estimated values. The agreement is reasonable and we believe that the true TCS values should not differ much from these findings.

Comparison with other results for electron-tetrahydropyran scattering is at the moment impossible as no TCS data can be found in the literature. Unfortunately, our measurements for tetrahydropyran are temporarily suspended due to a movement of the laboratory.

V. CONCLUDING REMARKS

We have measured the absolute TCS for trimethylene oxide, c-$(CH_2)_3O$, molecules from low to intermediate energies, 1–400 eV, using an electron-transmission method. To our best knowledge, these TCS results are the first reported. The experimental TCS energy dependence exhibits two distinct features: Below 3 eV it rises steeply toward lowest energies applied, and it has a broad enhancement spanned between 5 and 12 eV. Some weak resonantlike structures are also discernible: The small peak centered around 4 eV, and two weak bumps located near 6 and 8 eV, superimposed on the ridge of the enhancement. To resolve the origin of these features, more detailed experimental and theoretical studies are necessary.

In addition, the integral ECS and ICS have been computed for c-$(CH_2)_3O$ and c-$(CH_2)_5O$ molecular targets at intermediate and high electron-impact energies. The sum of ECS and ICS for c-$(CH_2)_3O$ agrees well with the experimental TCS at overlapping energies above 45 eV.

Comparison of the experimental TCSs for heterocyclic $(CH_2)_nO$, n=2–4, molecules has also been made and similarities and differences have been pointed out and discussed. Based on our intermediate-energy TCS measurements for this target series, we have decomposed the molecular TCSs into portions coming from constituent groups: CH_2 and O. By applying these effective partial TCS contributions, we have estimated the TCS for tetrahydropyran, c-$(CH_2)_5O$, the next member of the cyclic-ether family. The estimated TCS is in reasonable agreement with the present calculations.

ACKNOWLEDGMENTS

This work is part of the MNSzW program 2007–2008 and is supported by the Polish Ministry of Science and Higher Education (Project No. N202 110 32/2862). Numerical calculations have been performed at the Academic Computer Center (TASK) in Gdańsk.

[1] *Photon and Electron Interactions with Atoms, Molecules and Ions*, Landolt-Börnstein New Series Group I, Vol. 17, Pts. A–C, edited by Y. Itikawa (Springer, Berlin, 2000).
[2] *Advances in Atomic, Molecular, and Optical Physics*, edited by M. Kimura and Y. Itikawa (Academic, San Diego, 2001), Vol. 44.
[3] L. G. Christophorou and J. K. Olthoff, *Fundamental Electron Interactions with Plasma Processing Gases* (Kluwer, New York/Plenum, New York, 2004).
[4] Cz. Szmytkowski, P. Możejko, and G. Kasperski, J. Phys. B **31**, 3917 (1998); Cz. Szmytkowski and P. Możejko, Vacuum **63**, 549 (2001).
[5] M. Knudsen, Ann. Phys. **31**, 205 (1910).
[6] B. Bederson and L. J. Kieffer, Rev. Mod. Phys. **43**, 601 (1971).
[7] Cz. Szmytkowski, P. Możejko, and G. Kasperski, J. Phys. B **30**, 4363 (1997).
[8] R. N. Nelson and S. O. Colgate, Phys. Rev. A **8**, 3045 (1973).
[9] N. F. Mott and H. S. W. Massey, *The Theory of Atomic Collisions* (Oxford University Press, Oxford, 1965).
[10] Y.-K. Kim and M. E. Rudd, Phys. Rev. A **50**, 3954 (1994); W. Hwang, Y.-K. Kim, and M. E. Rudd, J. Chem. Phys. **104**, 2956 (1996).
[11] P. Możejko, B. Żywicka-Możejko, and Cz. Szmytkowski, Nucl. Instrum. Methods Phys. Res. B **196**, 245 (2002).
[12] F. Salvat, J. D. Martinez, R. Mayol, and J. Parellada, Phys. Rev. A **36**, 467 (1987).
[13] N. T. Padial and D. W. Norcross, Phys. Rev. A **29**, 1742 (1984).
[14] J. P. Perdew and A. Zunger, Phys. Rev. B **23**, 5048 (1981).
[15] X. Zhang, J. Sun, and Y. Liu, J. Phys. B **25**, 1893 (1992).
[16] M. J. Frisch, G. W. Trucks, H. B. Schlegel *et al.*, GAUSSIAN 03, revision B.03, Pittsburgh, PA, Gaussian Inc.
[17] L. S. Cederbaum, J. Phys. B **8**, 290 (1975).
[18] W. von Niessen, J. Schirmer, and L. S. Cederbaum, Comput. Phys. Rep. **1**, 57 (1984).
[19] J. V. Ortiz, J. Chem. Phys. **89**, 6348 (1988).
[20] V. G. Zakrzewski and W. von Niessen, J. Comput. Chem. **14**, 13 (1993).
[21] Y. Itikawa, Int. Rev. Phys. Chem. **16**, 155 (1997).

MOST WIEDZY Downloaded from mostwiedzy.pl
26 February 2024 10:59:09

[22] M. Allan and L. Andric, J. Chem. Phys. **105**, 3559 (1996).
[23] Cz. Szmytkowski, A. Domaracka, P. Możejko, and E. Ptasińska-Denga, Phys. Rev. A **75**, 052721 (2007).
[24] M. Kimura, O. Sueoka, A. Hamada, and Y. Itikawa, Adv. Chem. Phys. **111**, 537 (2000).
[25] K. Floeder, D. Fromme, W. Raith, A. Schwab, and G. Sinapius, J. Phys. B **18**, 3347 (1985).
[26] H. Nishimura and H. Tawara, J. Phys. B **24**, L363 (1991).
[27] Cz. Szmytkowski and S. Kwitnewski, J. Phys. B **35**, 2613 (2002).
[28] C. Makochekanwa, H. Kato, M. Hoshino, H. Cho, M. Kimura, O. Sueoka, and H. Tanaka, Eur. Phys. J. D **35**, 249 (2005).
[29] Cz. Szmytkowski and S. Kwitnewski, J. Phys. B **35**, 3781 (2002); **36**, 2129 (2003); **36**, 4865 (2003).
[30] P. Możejko, E. Ptasińska-Denga, A. Domaracka, and Cz. Szmytkowski, Phys. Rev. A **74**, 012708 (2006).
[31] *Handbook of Chemistry and Physics*, 76th ed., edited by D. R. Lide (CRC, Boca Raton, 1995).
[32] L. G. Christophorou and A. A. Christodoulides, J. Phys. B **2**, 71 (1969).
[33] Cz. Szmytkowski, A. Domaracka, P. Możejko, and E. Ptasińska-Denga, J. Phys. B **41**, 065204 (2008).
[34] S. Altshuler, Phys. Rev. **107**, 114 (1957).
[35] A. Zecca, C. Perazzolli, and M. J. Brunger, J. Phys. B **38**, 2079 (2005).
[36] M. Allan, J. Phys. B **40**, 3531 (2007).
[37] C. S. Trevisan, A. O. Orel, and T. N. Rescigno, J. Phys. B **39**, L255 (2006).
[38] C. Winstead and V. McKoy, J. Chem. Phys. **125**, 074302 (2006).
[39] D. Bouchiha, J. D. Gorfinkiel, L. G. Caron, and L. Sanche, J. Phys. B **39**, 975 (2006).
[40] S. Tonzani and C. H. Greene, J. Chem. Phys. **125**, 094504 (2006).
[41] M. Lepage, S. Letarte, M. Michaud, F. Motte-Tollet, M.-J. Hubin-Franskin, D. Roy, and L. Sanche, J. Chem. Phys. **109**, 5980 (1998).
[42] M. Dampc, I. Linert, A. R. Milosavljević, and M. Zubek, Chem. Phys. Lett. **443**, 17 (2007).
[43] A. Charlier, R. Setton, and M.-F. Charlier, Phys. Rev. B **55**, 15537 (1997).
[44] K. J. Miller, J. Am. Chem. Soc. **112**, 8533 (1990).
[45] M. Inokuti, Rev. Mod. Phys. **43**, 297 (1971); M. Inokuti and M. R. C. Mc Dowell, J. Phys. B **7**, 2382 (1974) (and references therein).
[46] G. Garcia and F. Manero, Phys. Rev. A **57**, 1069 (1998); Chem. Phys. Lett. **280**, 419 (1997); G. Garcia and F. Blanco, Phys. Rev. A **62**, 044702 (2000) (and references therein).
[47] Cz. Szmytkowski, Z. Phys. D: At., Mol. Clusters **13**, 69 (1989).
[48] W. M. Ariyasinghe, P. Wickramarachchi, and P. Palihawadana, Nucl. Instrum. Methods Phys. Res. B **259**, 841 (2007).
[49] M. Vinodkumar, C. Limbachiya, K. Korot, and K. N. Joshipura, Eur. Phys. J. D **48**, 333 (2008).
[50] Cz. Szmytkowski, Ł. Kłosowski, A. Domaracka, M. Piotrowicz, and E. Ptasińska-Denga, J. Phys. B **37**, 1833 (2004).
[51] G. Sunshine, B. B. Aubrey, and B. Bederson, Phys. Rev. **154**, 1 (1967).
[52] F. A. Baiocchi, R. C. Wetzel, and R. S. Freund, Phys. Rev. Lett. **53**, 771 (1984); M.-T. Lee, 14th International Symposium on Electron-Molecule Collisions and Swarms, Campinas, 2005, edited by S. d'A. Sanchez, R. F. da Costa, and M. A. P. Lima (unpublished), p. 74.

26 February 2024 10:59:09
MOST WIEDZY Downloaded from mostwiedzy.pl